Available online at www.sciencedirect.com
SCIENCE DIRECT
Catalysis Today 107–108 (2005) 346–354
CATALYSIS TODAY
www.elsevier.com/locate/cattod

Effect of support composition on hydrogenolysis of thiophene and Maya crude

Mohan S. Rana *, M.L. Huidobro, J. Ancheyta, M.T. Gómez

Instituto Mexicano del Petróleo, Eje Central Lázaro Cárdenas 152, Ciudad de México 07730, Mexico

Available online 22 August 2005

Abstract

The effects of support composition and molybdenum content have been investigated in order to determine their influence on hydrodesulfurization (HDS) catalytic process. The catalysts were characterized by BET specific surface area (SSA), pore volume (PV), pore size distribution (PSD), X-ray diffraction (XRD), in situ Fourier transform infrared (FTIR) and temperature-programmed reduction (TPR). Hydrodesulfurization (HDS) of thiophene model molecule reaction was carried out in a micro-catalytic reactor at 400 °C and atmospheric pressure. Sulfided catalysts showed a wide range of activity variation as a function of support composition which established that molybdenum sulfided active phases strongly depend on the nature and composition of support. The incorporation of MgO, SiO_2, TiO_2 and ZrO_2 with γ-Al_2O_3 alters the nature of active phase interaction on the support surface. Therefore, these oxides play a structural promoting role to the support contribution and its interaction towards the active metal geometry. With the variation of Mo loading on Al_2O_3-ZrO_2 the activities increase up to 12 wt.% Mo loading and after that activity remains constant with further increase in Mo content. The characterization results are in good agreement with MoO_3 monolayer formation. An Al_2O_3-ZrO_2 mixed oxide supported catalyst was tested at high pressure with real feed (Maya heavy oil) and the activity results were compared with a reference catalyst. The laboratory prepared catalyst was found slightly better selective for HDM than the reference catalyst, which is mainly due to the small amount of ZrO_2 mixed with alumina.

Keywords: Support effect; HDS; HDM; MgO-Al_2O_3; ZrO_2-Al_2O_3; SiO_2-Al_2O_3; TiO_2-Al_2O_3 mixed oxides supported catalysts; Maya crude

1. Introduction

The sulfur specification is tightening day by day and its content in diesel fuel will be less than 15 wppm by 2010 over the world. Hydrotreating is the most common process to reduce sulfur concentration in petroleum distillates, however, with the present catalysts and processes it is really hard to achieve the future sulfur specification. Therefore, refiners are looking for new catalysts with better activity as well as with improved product selectivity. There have been various attempts to improve catalyst activity such as changes in active metal composition, use of different types of active metals, additives and supports, etc. Among them the variation of support composition is one of the most promising approaches [1]. Significant results have been recently obtained with mixed oxide supported catalysts [2–7]. To reach the aforesaid specification, different mixed oxide amorphous and crystalline materials have been employed as supports for hydrotreating catalysts. MgO, SiO_2, TiO_2, ZrO_2 and their mixed oxides with Al_2O_3 have been reported to possess interesting range of textural properties as well as different kind of active metal interactions with the support [8]. The effect of support on catalyst activity has already been subject of several papers [9–17] and the authors have their efforts on studying different physical and chemical properties of the support mainly active metal characterization. However, few studies have been concentrated on the acidic and basic natures of the support and its effect on the nature of interaction with the active metal [18–20].

Generally, single oxide supported catalysts are known to be low active for hydrotreating functionalities compared with conventional γ-Al_2O_3 supported catalysts [15]. It is believed that active metal oxides (MoO_3, CoO and NiO)

* Corresponding author. Tel.: +52 55 9175 8418; fax: +52 55 9175 8429.
E-mail address: msingh@imp.mx (M.S. Rana).

0920-5861/$ – see front matter © 2005 Elsevier B.V. All rights reserved.
doi:10.1016/j.cattod.2005.07.029

interact in different manner with the support and consequently vary the dispersion of active metals [8]. Whereas mixed oxide supported catalysts generate favorable morphology of active phases, which also improve metal support interaction and fascinate the reducibility or sulfidability [1]. Apart from this, the cost of changing the support to improve catalyst behavior would be relatively lower compared with major changes of process parameters such as increase of H_2 partial pressure, reduction of space velocity and/or raise of reactor temperature.

This article summarizes the results of a work carried out to understand the effect that acidic and basic natures of different mixed oxides supported catalyst has on hydrotreating reactions. The support composition structurally promotes the catalytic functionalities by modifying the metal support interactions. The effect of support on the performance of promoted catalysts is evaluated with thiophene hydrodesulfurization (HDS) as well as with heavy oil (Maya crude) HDS and hydrodemetallization (HDM).

2. Experimental

2.1. Preparation of support

Mixed oxide supports were prepared by *homogeneous delayed precipitation* method using aqueous 10% NH_3 (NH_4OH) solution as a precipitating agent and controlling the pH at ≈8.5 in presence of stirring (800 rpm). The stirring was continuous for 4 h to allow the complete mixing of precipitates. The precipitation was digested overnight (∼15 h) and filtered with the required amount of distilled water to wash the nitrate and chloride ions. The material was dried at room temperature and subsequently at 120 °C for 12 h. The supports were finally calcined at 550 °C for 4 h. The mixed oxide samples were labeled as: PA (Al_2O_3), PS (SiO_2), AM (90 wt.% Al_2O_3-10 wt.% MgO), AS (90 wt.% Al_2O_3-10 wt.% SiO_2), AT (90 wt.% Al_2O_3-10 wt.% TiO_2) and AZ (90 wt.% Al_2O_3-10 wt.% ZrO_2). The compositions of supports were determined by atomic absorption and data are given in Table 1.

2.2. Preparation of catalyst

The molybdenum-supported catalysts were prepared by the incipient wetness impregnation method. An appropriate amount of ammonium heptamolybdate (Fluka AR grade) was dissolved in water and ammonium hydroxide (pH ≈ 7.6 ± 0.2) solution for impregnation. The Co and Ni promoted catalysts were prepared by sequential impregnation procedure on Mo supported catalysts (dried at 120 °C and calcined at 400 °C for 4 h). The cobalt and nickel nitrate salts were impregnated in aqueous medium. The final catalysts were dried at 120 °C overnight, and calcined in presence of air at 450 °C for 4 h.

2.3. Characterization of support and catalyst

BET SSA, pore volume and PSD measurements were carried out in a Quantachrome Nova 2000 equipment by nitrogen adsorption (−196 °C). Prior to the adsorption, the supports and catalysts were outgassed for 3 h at 300 °C. X-ray powder diffraction spectra were obtained using a Siemens D500 diffractometer in a 2θ range of 10–70° at 2.5° min^{-1} scan rate using Cu Kα radiation. Atomic absorption analyses were carried out in a SOLAAR-AA Series spectrometer using an air–C_2H_2 flame (2300 °C) for Ni and Co, and C_2H_2–NO_2 flame (3000 °C) for Mo. The solutions of samples were previously digested at 200 °C and 15–20 kg/cm^2 for 20 min, on a CEM-Mars 5 microwave oven.

For IR spectroscopic studies, two different probe molecules were used such as CO_2 and pyridine for supports and sulfided catalysts, respectively. The catalysts were sulfided at 400 °C for 2 h before probe molecule adsorption. Adsorptions of probe molecules were carried out at room temperature. The pyridine adsorbed samples were heated at different temperatures so changes in acidity could be observed as function of temperature. For temperature-programmed reduction (TPR) analyses, an Altamira AMI-3 instrument was used. A 20 mg sample of each promoted catalyst was reduced in a stream of H_2/Ar (10/90) at a flow rate of 30 mL/min, from 30 to 1000 °C, analyzing the off gas by TCD. Prior to each measurement the sample was preheated in a stream of Ar at 450 °C for 30 min to remove adsorbed water.

2.4. Hydrodesulfurization of thiophene

In a typical experiment about 100 mg of oxidic catalyst (0.4–0.8 mm size) was loaded into the reactor (0.8 cm i.d.). Prior to the activity test, the catalyst was sulfided at 400 °C

Table 1
Composition and textural properties of mixed oxide supports calcined at 550 °C

Sample	$Al_2O_3/(Al_2O_3 + x)$ (g g^{-1})	Na_2O (%)	Textural properties		
			SSA (m^2/g)	PV (mL/g)	APD (nm)
AS	0.92	0.91	364	0.53	5.79
AT	0.92	–	246	0.43	6.94
AM	0.93	–	234	0.35	5.94
AZ	0.91	–	213	0.38	7.16
PA	1.0	–	242	0.40	6.57
PS	1.0[a]	0.60	381	0.72	7.53

[a] $SiO_2/(SiO_2 + x)$, x = MgO, SiO_2, TiO_2 and ZrO_2.

for 2 h with 8–10% H_2S flow using a fixed bed glass reactor. Thiophene HDS experiments were carried out at 400 °C and atmospheric pressure with a flow of H_2/C_4H_4S mixture of 100 mL/min using a saturator temperature of 5 °C in order to have around 4.7 mol% thiophene. The conversions of thiophene were kept below 15% to operate in differential regime. Reaction rates were calculated according to the equation $r = x(F/W)$, where r is the reaction rate of thiophene in mol h^{-1} g^{-1}, x the conversion, W the weight of the catalyst in grams and F is the initial flow rate of the reactant in mol h^{-1} [21].

2.5. Hydrotreating of real feed (Maya crude)

To evaluate the catalytic behavior with real feed, a catalyst (CoMo/AZ) was tested in a high pressure micro-reactor described elsewhere [22,23]. The feed for this experiment was prepared synthetically with hydrotreated Maya crude and diesel (50/50, w/w). Diesel was used as a solvent to avoid precipitation and gum formation during feed processing. The properties of the feed are presented in Table 2. Metals (Ni and V) in the feed and products were analyzed using flame atomic absorption spectrometry (D 5863-00a ASTM standard). Sulfur content was analyzed by ultra-violet fluorescence (D 5453-00 ASTM standard) while nitrogen was measured by oxidative combustion and chemiluminescence (D 4629-02 ASTM standard) at high temperature combustion in an oxygen rich atmosphere. Asphaltene is defined as the insoluble fraction in *n*-heptane.

Catalyst was sulfided in situ with a mixture of dimethyldisulfide (DMDS), straight-run gas oil (SRGO) and H_2 (1 wt.% DMDS + SRGO). The H_2S is produced by decomposition of DMDS in situ. The reactor was loaded with 10 mL volume of oxided catalyst with 3–5 mm extrudates size diluted with equal volume of SiC. After de-pressurizing the reactor to atmospheric pressure, the sulfiding stream containing ≈2.0 wt.% "S" was fed to wet the catalyst bed at room temperature. The reactor liquid was drained after 4 h and then the temperature was linearly rose from 30 to 120 °C (30 °C/h) and kept at this value for 2 h. The temperature was then increased until 150 °C at a rate of 30 °C/h, at 2.8 MPa and stayed 2 h, and then temperature rose until 260 °C and hold for 3 h. The final temperature of sulfidation was 320 °C and it was stabilized for 5 h at 2.8 MPa. After sulfidation, the flow was switched to the HDT feed and the following operating conditions were adjusted: temperature 380 °C, LHSV 1 h^{-1}, H_2/HC 356 m^3/m^3 and pressure 5.4 MPa [23].

Table 2
Feed composition and its characteristics

Properties	Feed composition
Density, 20/4 °C	0.851
Asphaltene (*n*-C_7 insoluble) (wt.%)	6.4
Elemental analysis (wt.%)	
C	83.2
H	9.5
N	0.128
S	0.89
Metals (wppm)	
Ni	18.9
V	81.7
(Ni + V)	100.6

3. Results and discussion

3.1. Properties of support

It is considered that with delayed precipitation of TiO_2, ZrO_2, SiO_2 and MgO particles are deposited on the surface of Al_2O_3. Therefore, the Al_2O_3 is precipitated first and then its analogues of mixed oxides. The supports used in this study were characterized for specific surface area, pore volume and pore size distribution using N_2 adsorption–desorption isotherms. The composition of support was quantitatively analyzed with atomic absorption. These characterization results are summarized in Table 1. All mixed oxide supports have high BET surface area, pore volume and meso-pore size distribution. Particularly, this type of pore size distribution is important for heavy crude hydroprocessing.

The mixed oxide supports were characterized using X-ray diffractograms after 550 °C calcinations and the results are shown in Fig. 1. To identify the mixed oxide phases XRD

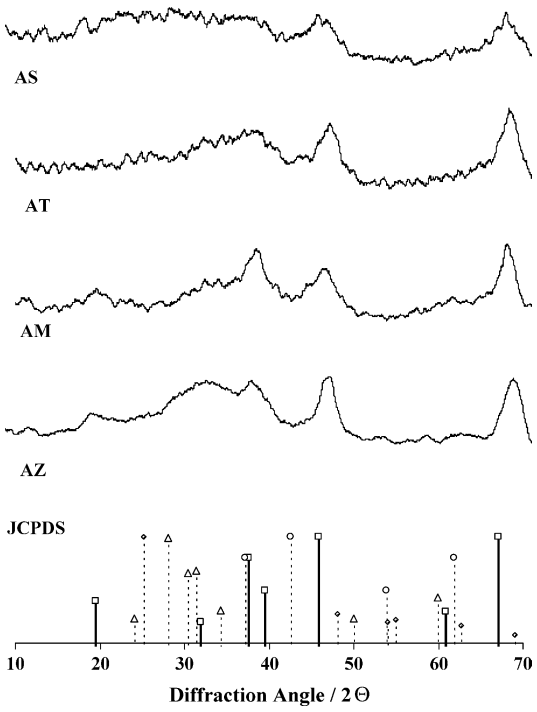

Fig. 1. X-ray diffractograms of mixed oxides supports and comparison with ASTM data: (□) γ-Al_2O_3-4-0875, (△) TiO_2-21-1272, (◇) ZrO_2-13-307 and (○) MgO-19-771.

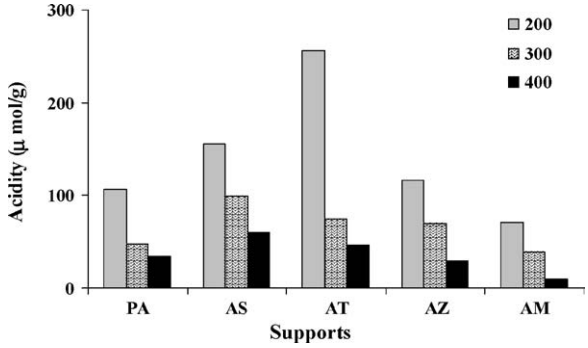

Fig. 2. Effect of support composition on Lewis acidity.

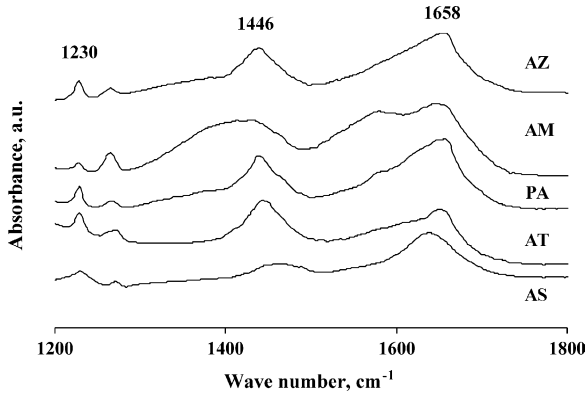

Fig. 3. Infrared spectra of CO_2 adsorption on different mixed oxide supports.

patterns were compared with the γ-Al_2O_3, MgO, ZrO_2 and TiO_2 of Joint Committee Powder Diffraction Standards (JCPDS) data [24]. The diffractograms are dominated with the γ-Al_2O_3 phases. It was observed from Fig. 1 that there were no peaks due to ZrO_2, TiO_2 and MgO. This may be due to the low concentration of these oxides or well dispersion of these oxides in the alumina matrix.

The quantitative pyridine adsorption–desorption data were obtained for different supports at different temperatures integrating the IR bands at 1598 and 1445 cm^{-1}, which are specific of vibration mode of pyridine interacting with the medium or weak Lewis acid sites [25]. Fig. 2 shows the pyridine desorption at different temperatures. Apart from the already mentioned bands there are other bands (1490, 1578 and 1616 cm^{-1}), and with the evacuation at higher temperature (<300 °C) the intensity of these bands diminishes completely. On the other hand, Brönsted acid sites were not detected, as indicated by the absence of a band at ca. 1540 cm^{-1}, characteristic of pyridinium species. Conversely, surface acidity was almost totally absent at 400 °C desorption for Al_2O_3-MgO and Al_2O_3-ZrO_2 supports, the increased density of Lewis sites in AS and AT supports is evident in the figure. These profound changes in acidity imply deep modifications on mixed oxides surface properties.

Fig. 3 shows different spectra of CO_2 adsorbed at equilibrium pressures on all mixed oxide supports. These spectra are indicative to the formation of carbonate (intense bands in the range 1200–1800 cm^{-1} assigned to $\nu_{ads}(CO_3)$ vibrations) and hydrogen carbonate species ($\nu(HCO_3^-)$ at 1230 cm^{-1}) [26,27]. Band positions are the same for all supports, indicating a similar strength of support basic centers (O^{2-} and OH groups). However, the integrated intensity of these bands is lower on AT and AS samples than on AM and AZ indicating basic nature of supports.

3.2. Characterization of catalysts

3.2.1. Composition, textural and structural properties of catalysts

The composition of the catalyst was determined by atomic absorption and the results are reported in Table 3. The Co(Ni) and Mo compositions remain more or less the same in all the catalysts or the difference is within the experimental error (i.e. ±0.3 and ±0.6% for Co(Ni) and Mo, respectively). Therefore, the comparison between the activities can be made based on the support effect or on the nature of the active sites existing in the catalyst. The physical properties of the promoted catalysts are also reported in the same table. The SSA and PV of the catalyst are in similar range except for AS. In the case of this catalyst SSA and PV are slightly higher than the others, which may have some effect on the activity [28].

Catalyst pore size distributions are shown in Fig. 4, indicating that all the catalysts contain meso type of pores. The AM supported catalyst showed bigger diameter of pores which may be due to the dissolution of MgO during the aqueous impregnation of Mo [14,22]. On the other hand, one

Table 3
Promoted catalyst composition and textural properties

Catalysts	Composition (wt.%)		Textural properties			Composition (wt.%)		Textural properties		
	Ni	Mo	SSA	PV	APD	Co	Mo	SSA	PV	APD
PA	3.1	7.6	213	0.31	5.9	3.6	7.1	202	0.31	6.2
PS	3.7	8.4	265	0.53	8.1	3.8	7.4	267	0.54	8.0
AT	3.5	8.6	214	0.33	6.3	3.9	7.8	216	0.34	6.3
AS	3.2	7.2	291	0.38	5.3	3.6	7.4	288	0.38	5.2
AM	3.8	8.5	196	0.31	6.3	3.7	7.9	193	0.31	6.3
AZ	3.1	7.6	210	0.33	6.4	3.6	7.2	211	0.33	6.2

SSA, m^2/g; PV, mL/g; APD, nm.

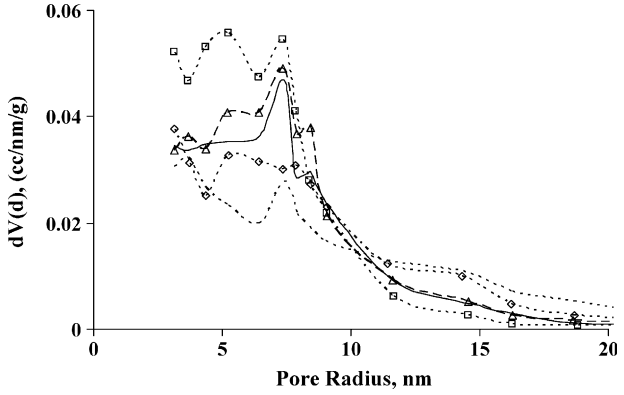

Fig. 4. Pore size distribution of CoMo supported catalysts: (—) CoMo/PA, (- - -) CoMo/AM, (□) CoMo/AS, (△) CoMo/AT and (◇) CoMo/AZ.

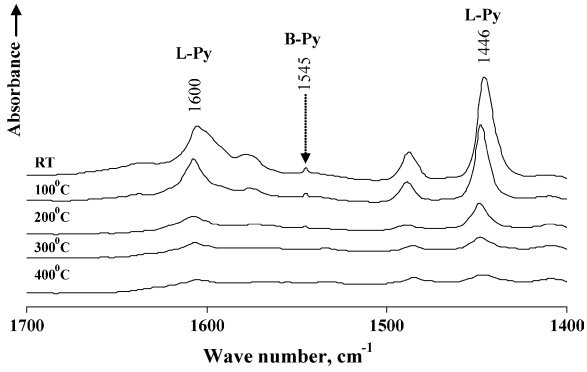

Fig. 6. FTIR spectra of pyridine at different temperatures over CoMo/γ-Al_2O_3 catalyst.

series of Mo variation (2–16 wt.%) was carried out in order to find out the monolayer formation on AZ, the textural properties of the catalysts are shown in Fig. 5. It is observed that surface area per gram of support remains constant up to 12 wt.% with Mo loading while the surface area per gram of catalyst decreases continuously. These results indicate that molybdenum oxide is in dispersed state on high surface area mixed oxides up to 12 wt.%. The decrease in surface area after 12 wt.% Mo loading is leading to the bulk metal oxide formation on the surface of the support. Therefore, on the basis of surface area and pore volume analyses it can be assumed that Mo exists as a monolayer up to 12 wt.% loading on AZ and after that due to the aggregation, bigger crystallite phases of MoO_3 are formed. However, with the XRD results (not shown) no crystalline phases were detected. These results suggested that MoO_3 crystals are well dispersed or the size is less than 4 nm which agree with previous results [29].

3.2.2. Adsorption of pyridine on the sulfided catalysts

The acidic properties of the sulfided catalysts were characterized using FTIR pyridine adsorption. The spectra of pyridine adsorbed on sulfided catalyst indicated very small amount of Brönsted acidity at 1541 cm^{-1} as shown in Fig. 6 for CoMo/Al_2O_3 catalysts at different temperatures. The evacuation at room temperature (RT) eliminates almost all the SH bond except for a very small band at 1544 cm^{-1}, which provides the evidence of protonated pyridine species (PyH^+) on the catalyst surface after contact with H_2S. These results are in good agreement with literature, which indicated that sulfided catalysts contain some Brönsted acid sites [21,25,30]. As for the quantitative acidity analysis of mixed oxide promoted catalysts, the IR bands at 1598 and 1445 cm^{-1}, which are specific to pyridine interacting with Lewis acid sites, decrease in the order AT ≈ AS > PA > AZ > AM as shown in Fig. 7. This order indicated that acidity of sulfided catalysts followed more or less similar trend as in pure support.

3.2.3. Temperature-programmed reduction

The qualitative TPR experiments were performed on different promoted catalysts to find out information about the interaction between active metal and supports. To evaluate this, promoted catalysts TPR are shown in Figs. 8–10. The comparison with SiO_2 was made due to its well-known properties to have low interaction with active phases [31]. In general, the reduction of MoO_3 species occurs in two steps ($MoO_3 \rightarrow MoO_2 \rightarrow Mo$). Thus, the peaks around 470 and 800 °C observed in the TPR profile can be assigned to the reduction of Mo^{6+} to Mo^{4+} [31–36]. The high temperature broad peaks at ca. 865 °C may be due to the dispersed tetrahedral Mo species. However, the peak

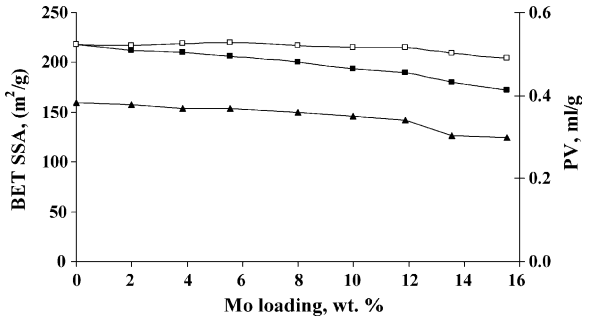

Fig. 5. Variation in specific surface area and total pore volume as a function of Mo loading on AZ: (□) surface area per gram of support, (■) surface area per gram of catalyst and (▲) pore volume.

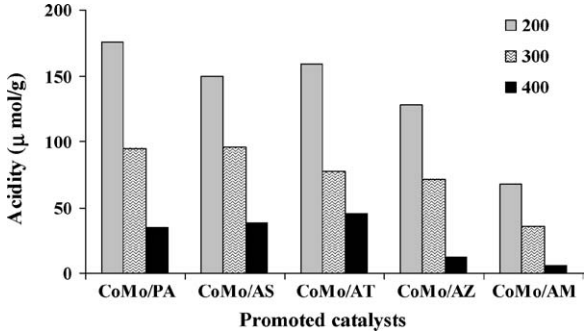

Fig. 7. Lewis acidity of sulfided CoMo catalysts as an effect of support composition.

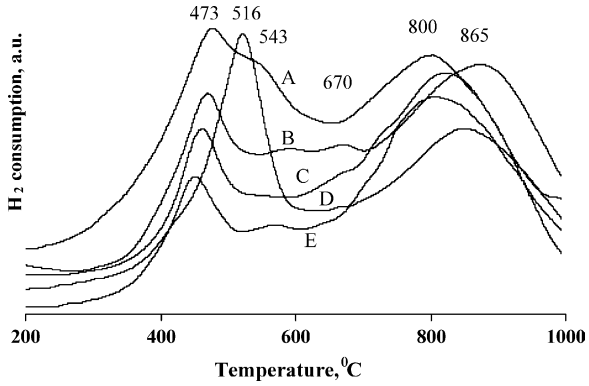

Fig. 8. CoMo supported catalysts TPR patterns on different supports: A (CoMo/AS), B (CoMo/AZ), C (CoMo/AT), D (CoMo/AM) and E (CoMo/PA).

at 865 °C is only observed for the case of AM and AZ supported catalysts, which are comparatively more basic than AT, AS and PA catalysts, due to the stronger interaction between support and active metals [36,37]. The peaks at different temperatures for different catalyst indicated that the support plays an important role on the reduction of Mo species [8]. An intermediate peak is observed at 530–700 °C which may correspond to the interaction between Co and Mo species.

On the other hand, in Fig. 9 NiMo supported catalysts showed at least three peaks in all samples. The first reduction peak appeared at low temperature (350–450 °C). In the case of AM this peak was observed at higher temperature (374 °C), indicating a stronger interaction between support and metals. The broad peaks at around 500–650 °C may exist due to the interaction between intermediate reducible species of Ni and Mo as well as Ni interaction with the support [18]. Particularly for AM the dissolution of MgO [22] plays an important role and the high temperature TPR results are in good agreement with literature reports [14] at ca. 914 °C. The low intensity of the peak may be due to the difference in preparation method and interaction of Mg ions

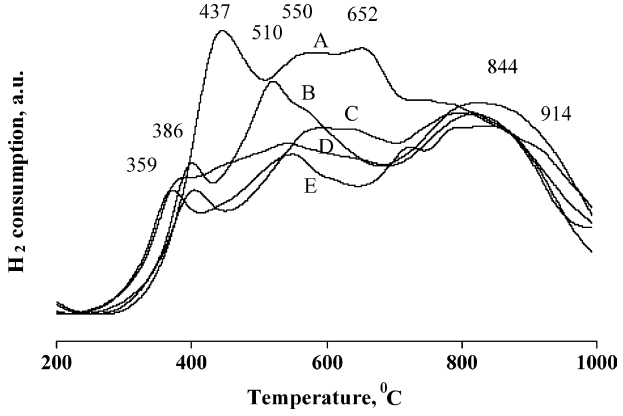

Fig. 9. NiMo supported catalysts TPR patterns on different supports: A (NiMo/AM), B (NiMo/AZ), C (NiMo/AS), D (NiMo/AT) and E (NiMo/PA).

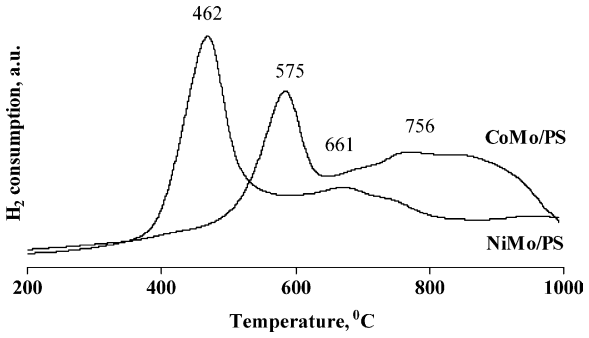

Fig. 10. TPR patterns of silica supported (NiMo/CoMo) catalysts.

with alumina. The high temperature broad peak for NiMo supported catalysts is observed at 845 °C for all the catalysts. In a comparison between CoMo and NiMo, the SiO_2 supported catalysts showed that low temperature peaks are dominated in both (NiMo and CoMo) cases by weak interaction while high temperature peak intensity is relatively low. Fig. 10 may also explain that the interaction of support also varies with active metal composition. However, the interactions of support depend on different parameters such as iso-electric point of support, impregnation pH as well as the number and strength of hydroxyl groups present on the surface of support [38,39]. These results may explain in some extent the different support interaction as well as the role of support in HDS activity.

3.3. Catalytic activity

3.3.1. Thiophene HDS

Catalytic activities with thiophene HDS were evaluated on the sulfided supported catalysts as function of Mo contents and the results are shown in Fig. 11. With the variation of Mo content the HDS rate increases up to 12 wt.% and after that it remains constant. The activity results are in good agreement with SSA and PV data which represent the oxidic monolayer formation on the surface. These results also corroborated that the oxidic monolayer remains unchanged after sulfidation. The linear increase in

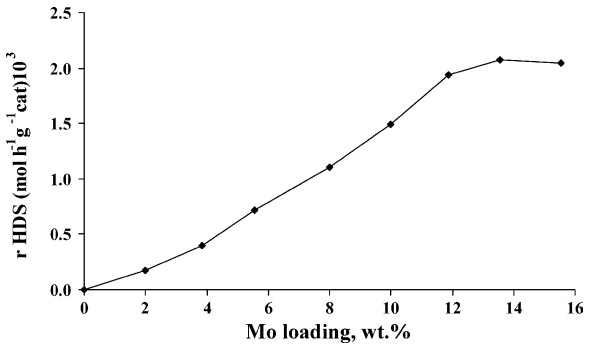

Fig. 11. Variation of thiophene reaction rate as a function of Mo loading on AZ.

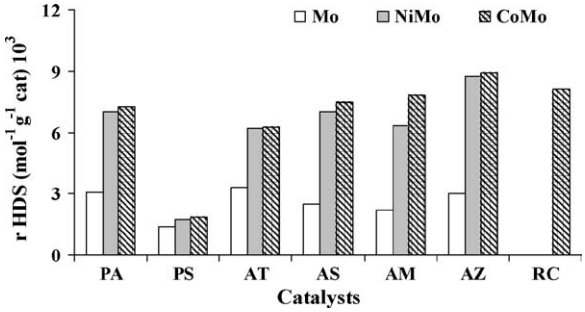

Fig. 12. Comparison of HDS rate as a function of support composition.

HDS activity indicated that the amount of anionic vacancies (coordinative unsaturated sites) increases on the sulfided catalysts accordingly. The HDS rate stands constant after 12 wt.% Mo loading, which indicates that above this loading the aggregation of Mo crystallite took place and as result the number of anionic vacancies remained constant or decreased.

A comparison of γ-Al_2O_3 mixed oxide supported catalysts is also shown in Fig. 12. These catalysts contain a Co(Ni)/[Co(Ni) + Mo] molar ratio around 0.43. With the variation of support composition the AZ promoted catalysts showed better activity than other mixed oxides. The comparison was also made with pure Al_2O_3 and SiO_2 supported catalysts as well as with a reference catalyst (RC) which contains TiO_2 in the support and higher amount of Mo. The activity variation suggests that anchoring of active sites on the surface of mixed oxide varies by changing the support composition. These results show that basic supported catalysts have better HDS activity than acidic ones or SiO_2 as well as alumina catalysts under these conditions. Thus, mixing of TiO_2, ZrO_2 and MgO with Al_2O_3 modifies the interaction behavior towards MoS_2, and since Co or Ni were expected to go to the edge of MoS_2, it can be said that the characteristics of the promoted catalysts are also altered [2,4]. Therefore, active sites that are responsible for catalytic functionalities are different in each catalyst and induce profound changes in activities. However, the role of surface area of these mixed oxides cannot be excluded. The TPR results are complementary to the activity results, which showed that basic nature of supported (AZ and AM) catalysts consumes more H_2 and showed higher temperature (at 865 °C) of reduction peak than the acidic supported ones.

Promotion of thiophene HDS activity of MoS_2 by Co and Ni is well reported as a support variation [19]. It can be seen from Fig. 12 that for un-promoted catalysts the observed effect of support is not very clear. The promoted catalyst showed better activity but the promotional effect is very low in comparison with ZrO_2 and MgO containing catalysts. The Ni and Co promoted activity increases by a factor of 2–3.5 except for the case of SiO_2. The relative increases for different supports are reported in Table 4. The low promotional effect may be due to the higher Co/(Co + Mo) ratio (i.e. 0.45), if we compare this value with the literature values [19,42] that contain molar ratio of 0.3, the decrease in Co on MoS_2 edge sites and the intrinsic promoting effect can be explained.

Table 4
Effect of support composition on promotional activities

Catalysts	Relative (Mo) increase	
	NiMo	CoMo
PA	2.3	2.4
PS	1.3	1.3
AT	1.9	1.9
AS	2.8	3.0
AM	2.9	3.5
AZ	2.9	3.0

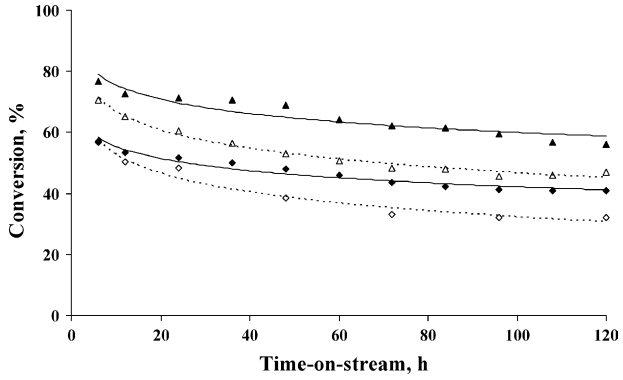

Fig. 13. HDS and HDM conversions with time-on-stream: (▲) RC-HDS (△) CoMo/AZ-HDS, (◆) RC-HDM and (◇) CoMo/AZ-HDM.

3.3.2. Maya crude HDS and HDM

It has been demonstrated that CoMo/AZ was the better catalyst for thiophene HDS, it was also tested against Maya crude hydrotreating and the activity results are reported with time-on-stream (TOS) in Fig. 13. The results are compared with the reference catalyst for HDS and HDM. The compositions of the fresh (CoMo/AZ and RC) and spent (CoMo/AZ-U and RC-U) catalysts are reported in Table 5. One more reason behind the selection of the ZrO_2 containing support for this study is the basic nature of support keeping silent features of textural properties from γ-alumina.

Table 5
Physical properties and composition of fresh and spent catalysts

Properties	CoMo/AZ (fresh catalyst)	CoMo/AZ-U (spent catalyst)	RC (fresh catalyst)	RC-U (spent catalyst)
Physical properties				
SSA (m^2/g)	209.5	69.2	152.2	132.9
PV (cm^3/g)	0.3277	0.1470	0.3579	0.2241
APD (nm)	6.26	5.50	9.40	6.74
Composition (wt.%)				
C	–	8.78		11.8
S	–	4.36		4.85
Ni	–	0.054	2.9	1.874
V	–	0.113		0.141
Co	3.56	2.93		–
Mo	7.64	5.19	11.4	5.116

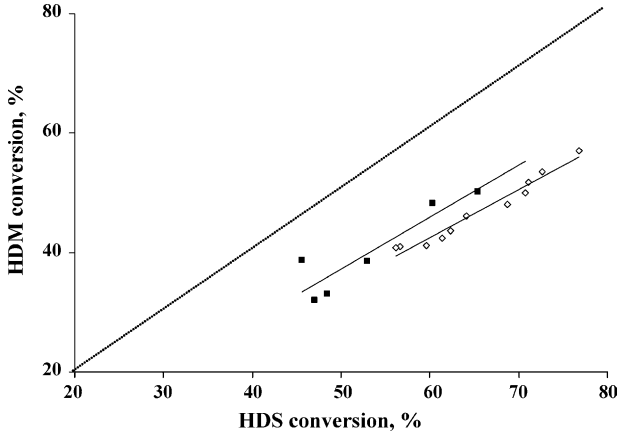

Fig. 14. HDM selectivity as an effect of feed composition: (■) CoMo/AZ and (◇) RC.

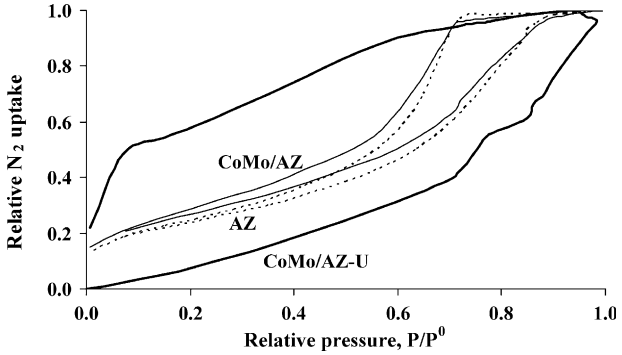

Fig. 15. A comparison of N_2 adsorption–desorption isotherms of support, fresh and spent catalysts.

The reference catalyst presented clearly better activity for HDS as well as HDM of Maya crude and exhibits more stability for HDM activity with TOS. Therefore, the nature of active sites behavior is different for model compounds and real feed. It seems that the larger pores in reference catalyst (Table 5) play an important role to make this difference in HDS and HDM activities. As a difference in HDS and HDM activities on AZ supported catalyst, the HDS active sites are considered more important than the textural properties, while for HDM the textural properties as well as the active sites seem to be important due to the diffusion of organo-metallic complex molecule into the pores [23]. It is observed with TOS that the relative HDS activity is parallel to the reference catalyst which decreases from 0.92 to 0.84, initial conversion to 120 h TOS, respectively. However, the AZ/RC ratio for HDM activity decreases faster than HDS activity that is 0.99–0.78 as initial (6 h) and final (120 h) conversion, respectively. In addition, these catalysts are selectively good for HDS as shown in Fig. 14. Obviously, the reference catalyst is slightly higher active but the AZ supported catalyst showed better selectivity for HDM. These results further indicate that heavy oil crude processing activity is not only due to the active sites but also some other properties such as pore size distribution are important to control the diffusion of molecules into the catalytic sites [40]. Interestingly, selectivity results showed that the basic nature of support is better for hydrogenolysis function but due to the smaller pore diameter the catalytic sites are restricted by pore mouth plugging. However, in the case of HDS the catalytic sites remain same as initial activity of the reference catalyst. On the other hand, the reference catalyst presents higher activity for HDS and which might be due to the effect of Ni containing catalyst [41–44] that promotes the deep HDS of sulfur molecules.

In regard to the deactivation, both PV and SSA were reduced by 60–80% in the case of spent catalysts, which showed extensive changes in the textural properties as presented in Table 5 and Fig. 15. This figure is a comparison of support, fresh catalyst and spent catalyst (CoMo/AZ-U) after 120 h TOS. Thus, the increase in area of hysteresis loop indicated that the pore plugging took place on the pore mouth. However, larger pore diameter has slower pore mouth plugging and better tolerance for metal retention. Indeed, "*ink-bottle*" types of pores are expected difficult to desorb until the relative pressure is quite low to allow the physicsorbed nitrogen from the narrow neck of pores.

4. Conclusions

High specific surface area mixed oxide support can be prepared using delayed co-precipitation of TiO_2, ZrO_2 and MgO with alumina. The characterization of acidic and basic natures of supports by pyridine and CO_2 adsorption indicated that the nature of support mainly depends on the nature of the delayed precipitated oxides such as MgO, ZrO_2 and TiO_2. The effect of support on thiophene HDS performance for Co(Ni)Mo catalysts is significantly affected by the nature (acidic and basic) of support, due to the different interaction with active phases. The promotional effect of Co and Ni on Mo supported catalysts is higher in the case of basic support than acidic one. TPR results showed that the basic supported catalysts have stronger metal support interaction than acidic supported ones. The high pressure HDT results on supported catalysts showed that the introduction of ZrO_2 in the Al_2O_3 provides better selectivity for hydrogenolysis function (HDM) with TOS due to the basic nature of support. The results indicate that ZrO_2 introduction indeed changes the number of active sites on MoS_2 and its promoted analogues. The spent catalyst textural properties showed that coke or metal sulfides deposition preferentially took place at the entrance of pores leading to 60–80% decrease in the specific surface area and total pore volume. An increase in adsorption–desorption area of isotherm represents the nature of pores in spent catalysts.

Acknowledgements

Two of us, M.L.H. and M.S.R., thank the Instituto Mexicano del Petróleo for financial support of a graduate

thesis and PDF, respectively. We express our appreciation to Mr. José G. Espinosa and Mrs. Bertha Nuñez for helping in preparation of feeds and adsorption–desorption experiments.

References

[1] Y. Okamoto, M. Breysse, G. Murali Dhar, C. Song, Catal. Today 86 (2003) 1.
[2] F. Luck, Bull. Soc. Chim. Belg. 100 (1991) 781.
[3] M. Breysse, P. Afanasiev, C. Geantet, M. Vrinat, Catal. Today 86 (2003) 5.
[4] H. Shimada, Catal. Today 86 (2003) 17.
[5] Y. Saih, K. Segawa, Catal. Today 86 (2003) 61.
[6] B. Pawelec, R.M. Navarro, J.M. Campos-Martin, A.L. Agudo, P.T. Vasudevan, J.L.G. Fierro, Catal. Today 86 (2003) 73.
[7] M.S. Rana, S.K. Maity, J. Ancheyta, G. Murali Dhar, T.S.R. Prasada Rao, Appl. Catal. A 268 (2004) 165.
[8] H. Shimada, T. Sato, Y. Yoshimura, J. Hiraishi, A. Nishijima, J. Catal. 110 (1988) 275.
[9] M.S. Rana, B.N. Srinivas, S.K. Maity, G. Murali Dhar, T.S.R. Prasada Rao, Stud. Surf. Sci. Catal. 127 (1999) 397.
[10] M.S. Rana, S.K. Maity, J. Ancheyta, G. Murali Dhar, T.S.R. Prasada Rao, Appl. Catal. A 253 (2003) 165.
[11] G. Murali Dhar, F.E. Massoth, J. Shatai, J. Catal. 85 (1984) 53.
[12] H. Topsøe, B.S. Clausen, F.E. Massoth, in: R.J. Anderson, M. Boudart (Eds.), Hydrotreating Catalysis—Science and Technology, vol. 11, Springer-Verlag, New York, 1996.
[13] M. Breysse, J.L. Portefaix, M. Vrinat, Catal. Today 10 (1991) 489.
[14] T. Klimova, D.S. Casados, J. Ramirez, Catal. Today 43 (1998) 135.
[15] G. Murali Dhar, M.S. Rana, S.K. Maity, B.N. Srinivas, T.S.R. Prasada Rao, in: C. Song, S. Hsu, I. Mochida (Eds.), Chemistry of Diesel Fuels, Taylor & Francis, London, 2000 (Chapter 8).
[16] S.K. Maity, M.S. Rana, B.N. Srinivas, S.K. Bej, G. Murali Dhar, T.S.R. Prasada Rao, J. Mol. Catal. A 153 (2000) 121.
[17] S.K. Maity, M.S. Rana, S.K. Bej, J. Ancheyta, G. Murali Dhar, T.S.R. Prasada Rao, Appl. Catal. A 205 (2001) 215.
[18] L. Qu, W. Zhang, P.J. Kooyman, R. Prins, J. Catal. 215 (2003) 7.
[19] Y. Ji, P. Afanasiev, M. Vrinat, W. Li, C. Li, Appl. Catal. A 257 (2004) 157.
[20] K.C. Pratt, J.V. Sanders, V. Christov, J. Catal. 124 (1990) 416.
[21] M.S. Rana, B.N. Srinivas, S.K. Maity, G. Murali Dhar, T.S.R. Prasada Rao, J. Catal. 195 (2000) 31.
[22] B. Caloch, M.S. Rana, J. Ancheyta, Catal. Today 98 (2004) 91.
[23] M.S. Rana, J. Ancheyta, P. Rayo, S.K. Maity, Catal. Today 98 (2004) 151.
[24] Powder Diffraction Files, JCPDS, International Central for Diffraction Data, 1969.
[25] F. Mauge, A. Sahibed-Dine, M. Gaillard, M. Ziolek, J. Catal. 207 (2002) 353.
[26] K. Segawa, W.K. Hall, J. Catal. 77 (1982) 221.
[27] W. Zmierzack, Q. Qader, F.E. Massoth, J. Catal. 106 (1987) 65.
[28] D. Wang, W. Qian, A. Ishihara, T. Kabe, J. Catal. 209 (2002) 266.
[29] F.E. Massoth, J. Catal. 36 (1975) 166.
[30] K. Segawa, W.K. Hall, J. Catal. 76 (1982) 133.
[31] EU Patent, 0181035 A2.
[32] A.J. Hegedus, K. Sasvari, J. Neugebauer, Z. Anorg, Allg. Chem. 293 (1957) 56.
[33] J.R. Regalbuto, J.-W. Ha, Catal. Lett. 29 (1994) 189.
[34] B. Scheffer, P. Arnoldy, J.A. Mouljin, J. Catal. 112 (1988) 516.
[35] P. Arnoldy, E.M. van Oers, O.S.L. Bruinsma, V.H.J. de Beer, J.A. Mouljin, J. Catal. 93 (1985) 231.
[36] P. Arnoldy, M.C. Franken, B. Scheffer, J.A. Mouljin, J. Catal. 96 (1985) 381.
[37] M. Kumar, F. Aberuagba, J.K. Gupta, K.S. Rawat, L.D. Sharma, G. Murali Dhar, J. Mol. Catal. A 213 (2004) 217.
[38] R. Prins, in: I.E. Wachs, L.E. Fitzpatrick (Eds.), Characterization of Catalytic Materials, Butterworth-Heinemann, USA, 1992 (Chapter 6).
[39] I.E. Waches, K. Segawa, in: I.E. Wachs, L.E. Fitzpatrick (Eds.), Characterization of Catalytic Materials, Butterworth-Heinemann, USA, 1992 (Chapter 4).
[40] S. Eijsbout, J.J.L. Heinerman, H.J.W. Elzerman, Appl. Catal. A 105 (1993) 69.
[41] T.C. Ho, Catal. Today 98 (2004) 3.
[42] F. Bataille, J.-L. Lemberton, P. Michaud, G. Perot, M. Vrinat, M. Lemaire, E. Schulz, M. Breysse, S. Kasztelan, J. Catal. 191 (2000) 409.
[43] S.H. Moon, Catal. Surv. Asia 7 (2003) 11.
[44] T. Isoda, S. Nagaro, X. Ma, Y. Korai, I. Mochida, Energy Fuels 10 (1996) 1078.